Supplementary Materials

G-quadruplex and G-rich sequence stimulate Pif1p-catalyzed downstream duplex DNA unwinding through reducing waiting time at ss/dsDNA junction

Supplementary Table S1. Sequences of substrates used in the experiments

	Sequences (5'-3') of substrates for single-molecule FRET
$s_{26}G4d_{17}$	AAGCAGTGGTATCAACGCAGAGAAAT(iCy3)GGGTTAGGGTTAGGGTTAGGGATGTATGACAAGGAAGG
$s_{26}G4d_{17}$*	(Cy3)AAGCAGTGGTATCAACGCAGAGAAATGGGTTAGGGTTAGGGTTAGGGATGTATGACAAGGAAGG
s_{26}4-G4d_{17}	AAGCAGTGGTATCAACGCAGAGAAAT(iCy3)GGGGTAGGGGTAGGGGTAGGGGATGTATGACAAGGAAGG
$s_{47}d_{17}$	(Cy3)T_{47}ATGTATGACAAGGAAGG
$GR_{47}d_{17}$	(Cy3)AAGCAGTGGTATCAACGCAGAGAAATGTGTGGTGTGTGTGTGTGGTGATGTATGACAAGGAAGG
$s_{26}d_{17}$	AAGCAGTGGTATCAACGCAGAGAAAT(iCy3)ATGTATGACAAGGAAGG
$GR_{26}d_{17}$	GTGTGTGTGGTGTGTGTGTGTGGTGT(iCy3)ATGTATGACAAGGAAGG
stem	Biotin-CCTTCCTTGTCAT(iCy5)ACAT
fork stem	Biotin-CCTTCCTTGTCAT(iCy5)ACATTAAATATATT
$d_{15}G4s_{17}$	ATAGGAAATAGGAGAGGGTTAGGGTTAGGGTTAGGGT(iCy3)T_{16}
stem	TCTCCT(iCy5)ATTTCCTAT-biotin
	Sequences (5'-3') of substrates for binding assay
FAM-GR_{12}	FAM-GTGTGTGTGGTG
FAM-T_{12}	FAM-TTTTTTTTTTTT
	Sequence (5'-3') of substrate for CD measurement
3G4	GGGTTAGGGTTAGGGTTAGGG
GR_{21}	GTGTGGTGTGTGTGTGTGGTG

Supplementary Table S2. Pif1p unwinds duplex DNA with very low activity

Substrates	Duplex length (bp)	Unwinding amplitude	References
overhang	16	~20%	(1,2)
	31	~0	(3)
fork	16	~30%	(2)
	20	~0	(4)

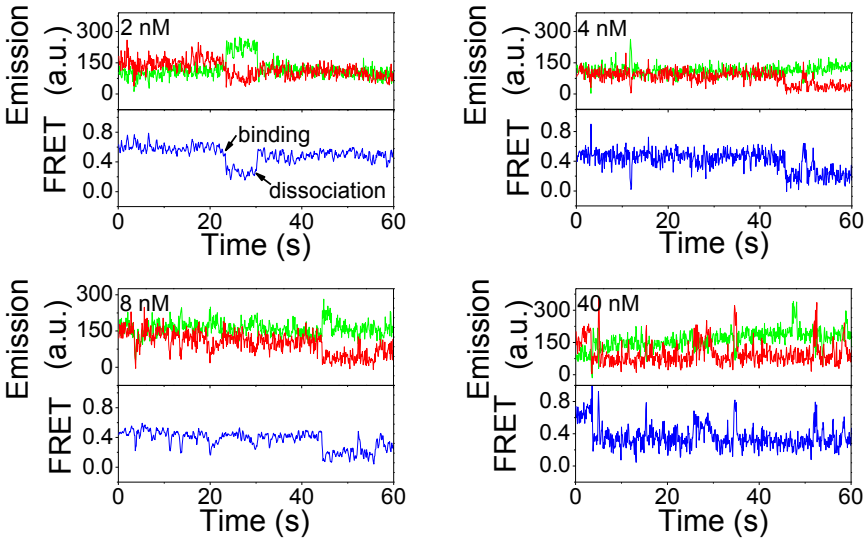

Supplementary Figure S1. Single-molecule fluorescence emission and FRET traces of interaction between ss/ds DNA $s_{47}d_{17}$ and 2-40 nM Pif1p. Those results show that Pif1p repetitively binds to and dissociation from the ss/ds DNA without duplex DNA unwinding.

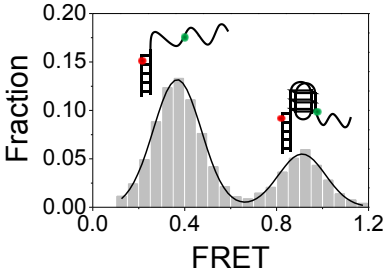

Supplementary Figure S2. FRET distribution before duplex unwinding for $s_{26}G4d_{17}$. The histogram can be well fitted by a double-peak Gaussian distribution with the two peaks at 0.37 and 0.91.

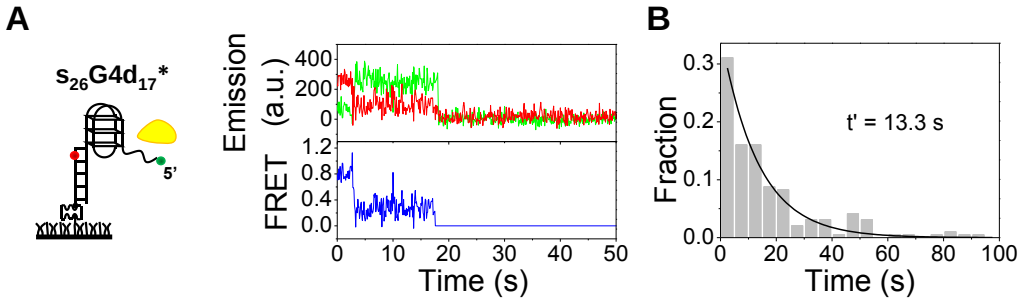

Supplementary Figure S3. Internal labeling of Cy3 at the 5' end of G4 does not influence the activity of Pif1p. (**A**) Construct of the $s_{26}G4d_{17}$* substrate in which the Cy3 dye was attached at the 5' end of the 26 nt ssDNA (left panel), and representative fluorescence emission and FRET traces for its unwinding (right panel, 80 nM Pif1p and 2 mM ATP). A waiting step still exists before the duplex DNA unwinding. Due to the longer distance between Cy3 and Cy5, the FRET values are lower than that for $s_{26}G4d_{17}$. (**B**) The waiting time follows a single-exponential distribution with a time constant of 13.3 s, similar to the 12.3 s value for $s_{26}G4d_{17}$. This result indicates the waiting time is not influenced by the internal labeling of Cy3 in $s_{26}G4d_{17}$.

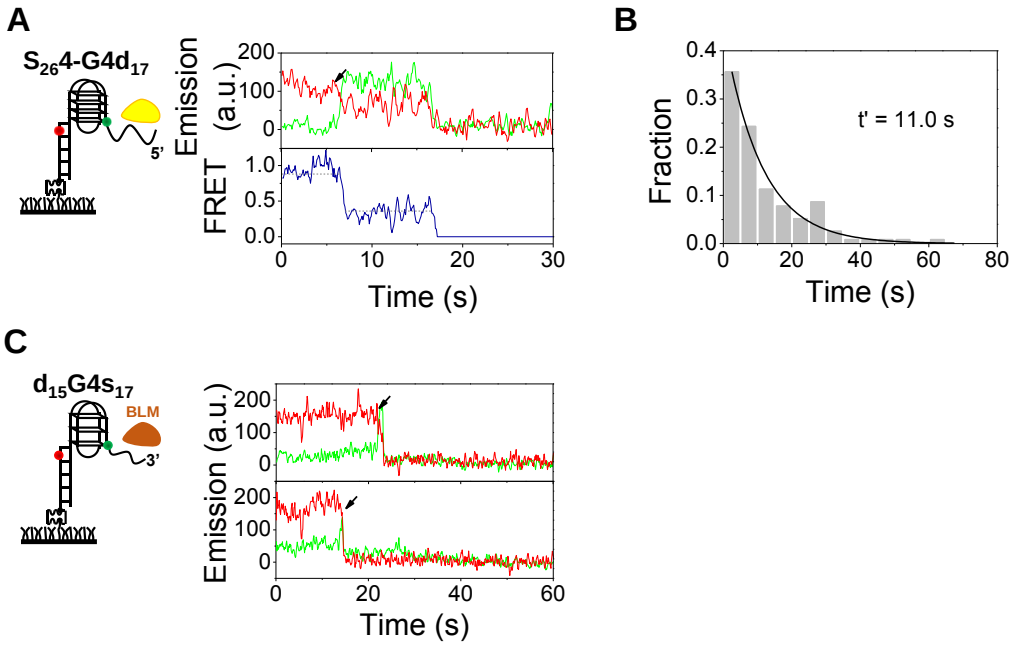

Supplementary Figure S4. Pif1p has a waiting step during the unwinding of different G4/duplex DNA. (**A**) Representative fluorescence emission and FRET traces for the unwinding of s_{26}4-G4d_{17} DNA. The arrow indicates the addition of Pif1p and ATP. (**B**) Histogram of the waiting time follows an exponential decay with a time constant of 11.0 s. (**C**) Representative fluorescence emission traces for BLM unwinding of d_{15}G4s_{17} DNA. Black arrows indicate the continuous unfolding of G4 and unwinding of the downstream duplex DNA.

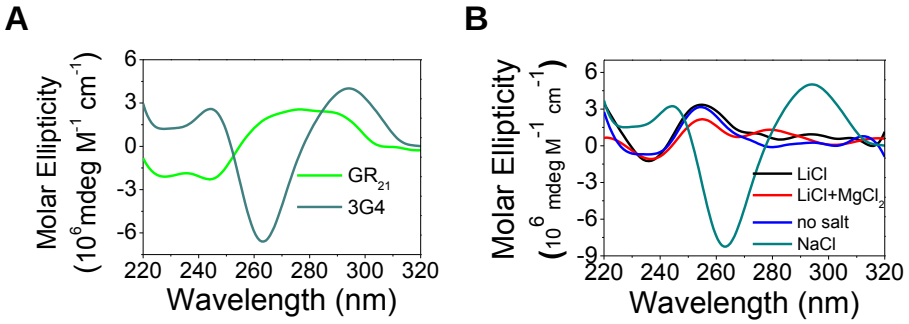

Supplementary Figure S5. CD measurements to examine the formation of G4 structures. (A) This result shows that no G4 structure is formed for the G-rich sequence GR_{21}. (**B**) CD measurements of G4-forming sequence 3G4 in different buffer conditions indicate no G4 structure is formed in 50 mM LiCl and 10 mM $MgCl_2$.

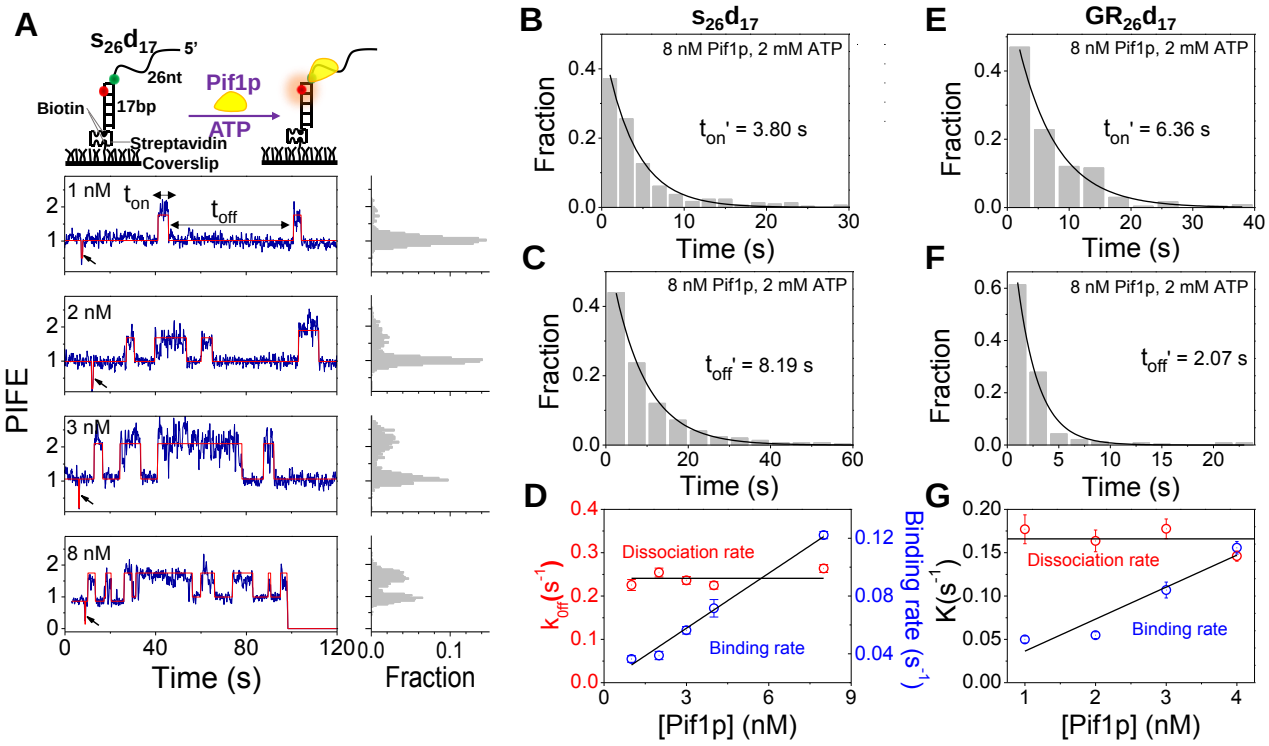

Supplementary Figure S6. Concentration dependence of Pif1p binding to partial duplex DNA. (**A**) Schematic representation of experimental procedures, and representative traces and histograms of Pif1p binding to $s_{26}d_{17}$ with increasing concentrations of Pif1p at 2 mM ATP. Unbound DNA has a normalized PIFE value of 1. Once Pif1p binds to DNA, PIFE increases to ~2 as shown by the histograms. Blue curves are original traces, and red curves are traces fitted by a step-finding program. Black arrow indicates the addition of Pif1p and ATP. t_{on} is the dwell time for the helicase to remain bound to the DNA substrate and t_{off} is the time interval between two successive binding events. (**B, C**) Histograms of t_{on} (**B**) and t_{off} (**C**) distributions at 8 nM Pif1p for $s_{26}d_{17}$. t_{on}' and t_{off}' are the time constants from single-exponential fittings. The reciprocal of the two time constants correspond to the dissociation and binding rates of the helicase, respectively. (**D**) Effects of Pif1p concentration on the dissociation rate k_{off} ($1/t_{on}$) and binding rate of $s_{26}d_{17}$. As expected for a binary reaction, the dissociation rate is independent of Pif1p concentration while the binding rate has a linear dependence on it (5). The average dissociation rate is k_{off} = 0.24 s^{-1} and a linear fit of the binding rates at different Pif1p concentrations yields an binding rate constant of k_{on} = 1.3×10^7 $M^{-1}s^{-1}$. The dissociation constant of Pif1p is thus determined as $K_D = k_{off}/k_{on}$ = 18.5 nM. (**E-F**) Histograms of t_{on} and t_{off} distributions for Pif1p binding to $GR_{26}d_{17}$. t_{on}' (6.36 s) and t_{off}' (2.07 s) are the time constants from single-exponential fittings. It can be clearly seen that Pif1p binds more readily and tightly to G-rich sequence. (**G**) Effects of Pif1p concentrations on the dissociation rate (0.17 s^{-1}) and binding rate constant (3.7×10^7 $M^{-1}s^{-1}$) of $GR_{26}d_{17}$. The dissociation constant is thus determined as $K_D = k_{off}/k_{on}$ = 4.5 nM, lower than that for $s_{26}d_{17}$.

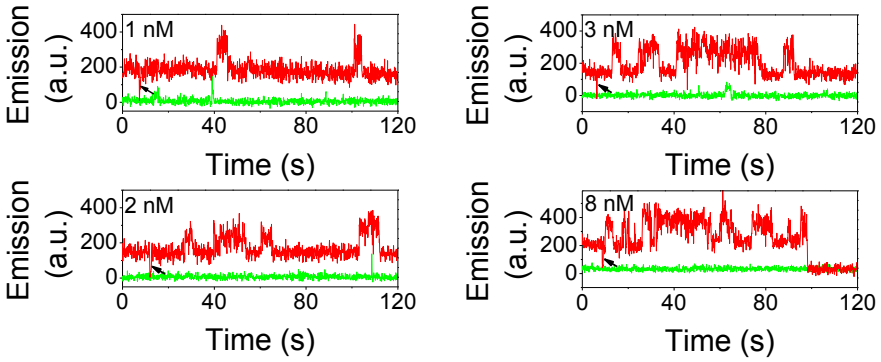

Supplementary Figure S7. Fluorescence emission traces for $s_{26}d_{17}$ in the presence of Pif1p at nanomolar range. Representative traces of Pif1p binding to $s_{26}d_{17}$ DNA with increasing concentrations of Pif1p at 2 mM ATP. Cy3 emission has a constant value close to the background. Cy5 emission shows repetitive enhancement, indicating approaching to the ss/dsDNA junction by Pif1p. The corresponding PIFE traces are shown in Supplementary Figure S6A.

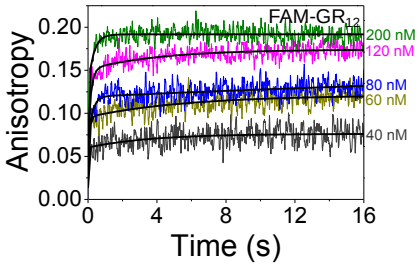

Supplementary Figure S8. Stopped-flow kinetic time-courses for Pif1p binding to a FAM-GR_{12}. The final concentration of FAM-labeled DNA was 40 nM and that of Pif1p was from 40 to 200 nM. Fluorescence signal was recorded upon addition of Pif1p. The initial binding time course was fitted to a double-exponential process: $y = y_0 - A_1\exp(-t/t_1) - A_2\exp(-t/t_2)$, where t represents the time, y represents the fluorescence anisotropy and y_0 is a constant. The two binding time constant t_1 and t_2 are shown in Figure 2E and F.

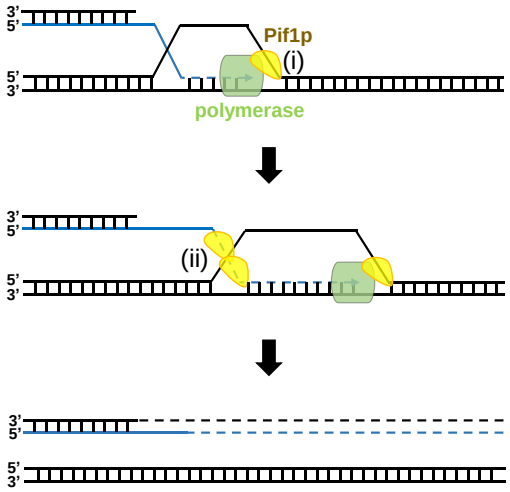

Supplementary Figure S9. Potential significances of G4/G-rich-stimulated duplex DNA unwinding. Telomeric DNA can be extended by ALT (alternative lengthening of telomeres). A D-loop is formed during DNA recombination. Pif1p promotes D-loop migration by: (i) the functional interaction with polymerase and (ii) displacing the newly synthesized DNA strand. Eroded telomeres or DNA breaks with 3'-G-rich tail may significantly stimulate the separation of new strand from template to promote DNA lengthening.

References:

1. Duan, X.-L., Liu, N.-N., Yang, Y.-T., Li, H.-H., Li, M., Dou, S.-X. and Xi, X.-G. (2015) G-quadruplexes Significantly Stimulate Pif1 Helicase-catalyzed Duplex DNA Unwinding. *J. Biol. Chem.*, **290**, 7722-7735.
2. Ramanagoudr-Bhojappa, R., Chib, S., Byrd, A.K., Aarattuthodiyil, S., Pandey, M., Patel, S.S. and Raney, K.D. (2013) Yeast Pif1 Helicase Exhibits a One-base-pair Stepping Mechanism for Unwinding Duplex DNA. *J. Biol. Chem.*, **288**, 16185-16195.
3. Zhou, R., Zhang, J., Bochman, M.L., Zakian, V.A. and Ha, T. (2014) Periodic DNA patrolling underlies diverse functions of Pif1 on R-loops and G-rich DNA. *eLife*, **3**, e02190.
4. Boulé, J.-B. and Zakian, V.A. (2007) The yeast Pif1p DNA helicase preferentially unwinds RNA–DNA substrates. *Nucleic Acids Res.*, **35**, 5809-5818.
5. Markiewicz, R.P., Vrtis, K.B., Rueda, D. and Romano, L.J. (2012) Single-molecule microscopy reveals new insights into nucleotide selection by DNA polymerase I. *Nucleic Acids Res.*, **40**, 7975-7984.